

Search for nuclearites by the satellite-based TUS air fluorescence detector

K. Shinozaki*, A. Montanaro, M. Bertaina, F. Fenu, S. Ferrarese,

University of Turin, Turin, Italy

E-mail: kenji.shinozaki@unito.it

P. Klimov, S. Sharakin, M. Zotov

*D.V. Skobeltsyn Institute of Nuclear Physics, M.V. Lomonosov Moscow State University,
Moscow, Russia*

A. Cellino, A. Castellina,

*INAF, National Institute for Astrophysics – OATO, Astrophysical Observatory of Turin, Pino
Torinese, Italy*

A. Anzalone

*INAF National Institute for Astrophysics – IASF, Institute of Space Astrophysics and Cosmic
Physics, Palermo, Italy*

R. Caruso

University of Catania, Catania, Italy

F. Isgro

University of Naples, Naples, Italy

Nuclearites are a hypothetical massive strange quark matter. They are supposed to be gravitationally trapped in Our Galaxy. Their absolute velocity is considered to be similar to that of the galactic rotation near the Sun. When the nuclearite traverses in the medium, a part of the energy loss is converted to the light radiation. This principle has been used for nuclearite searches made by underground or underwater neutrino observatories. In the night atmosphere, such an event form a meteor-like moving light spot. In the present work, we applied this detection method to search for nuclearites using the TUS (Tracking Ultraviolet Setup) instrument, the first orbital air fluorescence detector on the Lomonosov satellite launched in April 2016. The apparatus consisted of a ~ 2 m² segmented Fresnel reflector viewed by 256 photomultiplier tubes with readout electronics. TUS was operated in the meteor observation mode during the mission that allows the register luminous moving event with a time resolution of 6.6 ms. Since the area simultaneously observed by TUS in the orbit at ~ 485 km height, is on the order of ~ 6000 km² that provides a potential to accumulate exposures comparable to the former experiments within on the order of days. In the present contribution, we report the preliminary results of the first nuclearite search using the satellite-based air fluorescence detector and relevant simulation studies.

*36th International Cosmic Ray Conference -ICRC2019-
July 24th - August 1st, 2019
Madison, WI, U.S.A.*

*Speaker.

1. Introduction

The nature of the dark matter has been an open question in cosmology, particle physics, and relevant contemporary physics. Nuclearites are such a hypothetical strange quark matter (SQM) that are gravitationally bound in Our Galaxy [1]. SQM nuggets consisting of the equal numbers of up-, down-, and strange- quarks are stable for any baryon number, i.e., masses m ranging those of ordinary nuclei, macroscopic object, or even a neutron star. Being electrically neutral by captured electrons, they only lose energy in elastic collisions with atoms in the medium since Coulomb repulsion prevents nuclear interactions. A fraction of the energy is converted to the black-body radiation from an expanding cylindrical thermal shock wave.

So far, several experiments searched for nuclearites using various methods. First of all, the dark matter density near the Sun ρ_{DM} is 0.35 GeV cm^{-3} [2] or a similar order. This gives a limit on an isotropic flux of the nuclearites at a velocity v in the observer's frame to be $\rho_{\text{DM}}v/(4\pi mc^2)$. Reference [3] summarized the upper limits on the nuclearite fluxes in the earlier dates. The most stringent limit quoted as 'mica' was on the order of $\sim 10^{-20} \text{ cm}^{-2} \text{ sr}^{-1} \text{ s}^{-1}$ at a 90% confidence level that depended upon many assumptions. The underground MACRO experiment at Gran Sasso gave a limit to be $2.7 \times 10^{-16} \text{ cm}^{-2} \text{ sr}^{-1} \text{ sr}^{-1}$ above $3 \times 10^{14} \text{ GeV}/c^2$ ($\approx 2 \times 10^{-10} \text{ g}$) [4]. The ANTARES underwater neutrino observatory in the Mediterranean reported another limit to be $7 \times 10^{-17} \text{ cm}^{-2} \text{ sr}^{-1} \text{ s}^{-1}$ above $10^{17} \text{ GeV}/c^2$ ($\approx 0.2 \text{ }\mu\text{g}$) [5]. The last two are capable of detecting "slow-moving" light spot produced in the detector volume and of determining its 'light curve', kinematics, and geometry. In the atmosphere, a similar moving light spot is generated by the passage of the nuclearite. The radiation mechanism is similar to that of meteors. Compared with volume detectors, the atmosphere provides a huge target volume to search for nuclearites.

On April 28th, 2016, the TUS (Tracking Ultraviolet Setup) instrument [6] was launched as the first air 'fluorescence detector' (FD) operated in the orbit. The technique of FDs has been well established for detecting the extensive air shower (EAS) phenomenon initiated by the ultra-high energy cosmic rays (UHECRs) in the night atmosphere. The TUS telescope consisted of a mirror optics, photo-detectors at the focus, and ultra-fast readout electronics to collect faint UV fluorescence light emitted from the relativistic EAS particles. TUS was equipped with slower modes to detect the other light emission phenomena with different intensity and time scales. We exploit the data acquired in the "METEOR" mode to search for the nuclearite. With a $\sim 9^\circ$ field of view (FOV) equivalent to a $\sim 6000 \text{ km}^2$ ($6 \times 10^{13} \text{ cm}^2$) area, it had a potential of accumulating an exposure of the order of $10^{19} \text{ cm}^2 \text{ s sr}$ per ~ 1 -day observation time.

In the present work, we report the preliminary result of a nuclearite search by the first satellite-based air fluorescence detector. We introduce the descriptions of the detection principle and TUS instrument. Data analysis and simulations and models therein are mentioned throughout the text. In the end, we summarize the present work and future perspectives.

2. Nuclearites in the atmosphere

The principle of the nuclearite search by TUS is based on the detection of moving light spot in the atmosphere. The radiation mechanism of the nuclearites in the atmosphere and observable characteristics of such spots were modeled in Reference [1] for an assumed nuclearite velocity of

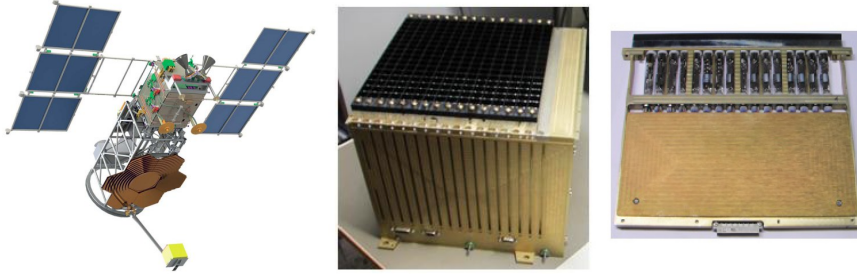


Figure 1: Left: artist's view of the TUS instrument on Lomonosov satellite. Middle: focal detector. Right: detector module.

to be 250 km s^{-1} as a typical radiation velocity of the Galaxy near the Sun. As the SQM density $\rho_N = 3.6 \times 10^{14} \text{ g cm}^{-3}$ is a constant, the cross sectional area σ_0 of a nuclearite with m is given to be $\pi \cdot \left[\sqrt[3]{4\pi\rho_N/(3m)} \right]^2 = 2.3 \times 10^{-10} [\text{cm}^2] \cdot (m/1 [\text{g}])^{2/3}$. For a given v , the energy loss rate per unit time in the medium with an density ρ are expressed as $-dE/dt = v \cdot dE/dl = \sigma_0 \rho v^3 \propto m^{2/3} v^3$. Above $\sim 0.1 \text{ g}$ nuclearites can penetrate the Earth's diameter. In the atmosphere, the conversion efficiency of the energy loss to the radiation is $\sim 4\%$ and is inverse proportional to the air density. In the present work, we applied small modifications on the formulae in the aforementioned reference to allow for arbitrary velocities. It yields a constant luminosity that is formulated in terms of the visible band apparent magnitude $V = 0.8 - \log(m/1 [\text{g}])^{5/3} - \log(v/250 [\text{km s}^{-1}])^{15/2} + 5 \log(r/1 [\text{km}])$ where r is the distance to the observer. For simplicity, we also assume that the flux is as the constant over the wavelength as that at 550 nm following the definition of the V-band magnitude.

Reference [1] also gave the maximum height where the nuclearite at $v = 250 [\text{km s}^{-1}]$ can effectively generate the light assuming a constant atmospheric scale height. We converted the corresponding air density ρ_{th} to convert the height using a realistic density profile function.

3. Apparatus

Figure 1 illustrates an artist's view of the TUS instrument seen in the lower part on the left panel. The photographs of the focal detector and an individual detector module on the middle and right panels, respectively. The TUS instrument is one of the scientific payloads on Mikhailo Lomonosov satellite (MVL-300). In a circular, sun-synchronous orbit with a 97.3° inclination, it has an average orbital speed of 7.6 km s^{-1} . The orbital period is $\sim 94 \text{ min}$. The height from the Earth's ellipsoid H ranges $470\text{--}502 \text{ km}$ with an average of 482 km .

The TUS telescope consisted of a $\sim 2\text{-m}^2$ reflector formed by seven hexagonal segmented Fresnel mirrors viewed with 256 channels with a Hamamatsu R1463 photomultiplier tube (PMT). Sixteen 'detector modules' controlled 16 PMTs each and supplied the high voltages (HVs) according to the background level. A light guide was deployed to form a square entrance of side 15 mm to lead photons to a 13 mm diameter the photocathode covered by a UFS1 band-pass filter. The plate scale was about 10 mrad ($\sim 0.6^\circ$) per channel side, equivalent to $\sim 5 \text{ km}$ projected on sea level.

Figure 2 shows the point spread function (PSF) from the ray trace simulations used in the present work. The left, middle, and right panels display for the parallel light rays from on-axis and 2° - and 4° -off-axis, respectively. Each quadrants in the panels corresponds to a channel area.

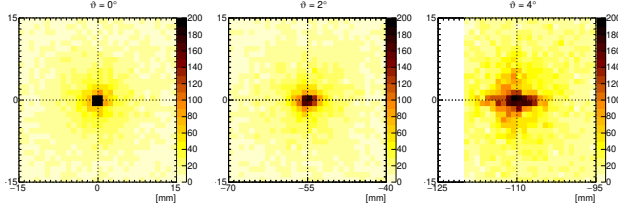


Figure 2: PSF of TUS optics. Left: on-axis. Middle: 2° -off-axis. Right: 2° -off-axis.

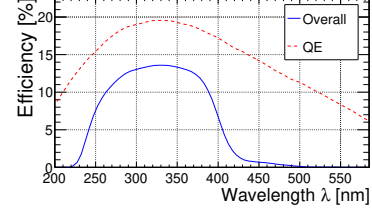


Figure 3: Overall efficiency and QE of PMT.

Figure 3 shows the quantum efficiency (QE) of the PMTs and the overall efficiency as a function of the wavelength. The latter includes transmittance of the filter and the reflectivity of the reflector. The efficiency of the optics system in terms the ratio of photon to be focused on the spot was measured to $\sim 70\%$. In the simulations, we conservatively assumed the reflectivity of the reflector and light guide to be this value.

In the present work, we used the “METEOR” data acquisition (DAQ) mode that registered signals in a ~ 6.6 ms time, called a (time) tick, over 256 ticks corresponding to ~ 1.68 s when a preset trigger condition was satisfied. DAQ ceased about 50 s after each trigger. As the main purpose of TUS was search for EAS events, this mode was operated in 36 limited discrete dates by the end of the mission’s last DAQ in November 2017.

4. Analysis

On acquired 34,749 METEOR mode data, we applied three selection levels: 0) 9825 events by the HV status indicating a nocturnal background levels, 1) 5057 events by requiring the sub-satellite point on the sea at least 75 km away from the nearest coast, and 2) 1665 events by Moon’s zenith angle $\Theta_{\text{moon}} > 90^\circ$. These criteria also apply the observation time when TUS was supposed to be active for DAQ. The Levels 1) and 2) cuts were for minimizing the effect of the anthropogenic light and eliminating direct moonshine on the focal detector, respectively.

The gains of the PMTs were estimated by the mean ADC counts $\langle \text{ADC}_0 \rangle$ and variance σ^2 of the background n_{pe} level. We assume that n_{pe} fluctuates only statistically, i.e. $\sigma^2 \propto n_{\text{pe}}$ for $\langle \text{ADC}_0 \rangle \propto n_{\text{pe}}$. These values were calculated from the ADC counts in the first 32 ticks of all the channels in the Level 2) data. We used the peak of the estimated G distribution for the analysis and simulations. About 200 PMTs were found in a reasonable gain of the order of 10^6 . These estimated gains and the subsequent results are preliminary.

Figure 4 shows an example of a METEOR mode event. Panels display: (a) ADC counts as a function of time tick, (b) estimated n_{pe} excess from the background levels, (c) sum of n_{pe} excess over 256 ticks on the focal detector, and (d) motion of the center of gravity of the excesses on the detector axes expressed in units of module and PMT numbers. Any channel with a $> 25\sigma$ excess of ADC counts at least in one tick above the level background are selected.

Panel (a) indicates the light curves of the raw data that also illustrate the different gain and background levels among the channels. Panel (b) shows the light curves as of n_{pe} excesses at a normalized gain of 10^6 . In Panel d), the linear fitting allows an estimation of the angular velocities $\vec{\omega}_{\text{MD}}$ and $\vec{\omega}_{\text{PM}}$ along both axes. Their composite $\vec{\omega} = \vec{\omega}_{\text{MD}} + \vec{\omega}_{\text{PM}}$ yields 0.17 rad s^{-1} and its

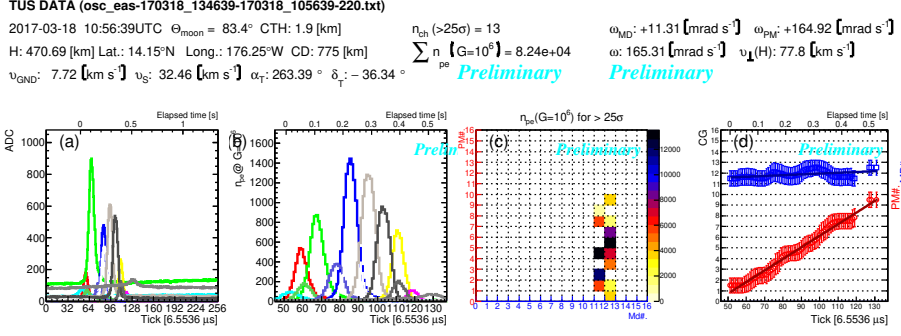


Figure 4: Example of a METEOR mode event: (a) ADC counts of the significant channels, (b) estimated n_{pe} , (c) estimated $\sum n_{pe}$ over all time-ticks on the focal detector, and (d) motion of the center of gravity of the significant signals. The channels with a $> 25\sigma$ excess are selected.

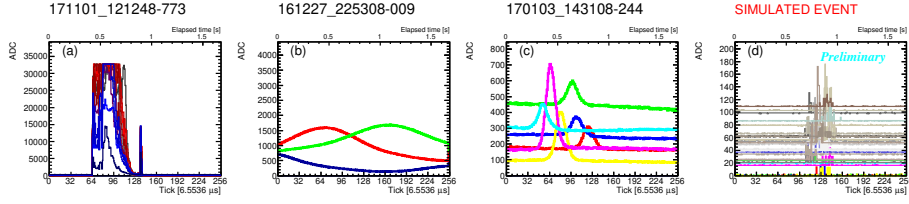


Figure 5: Example of light curves of events with a moving behavior: a) the event that almost all channels had saturated counts, b) signals from a supposed city light, and c) signals from a supposed meteor event. Panel d) displays for a simulated nuclearite event for comparison

orientation Ψ represents the projected nuclearite track on the FOV. By a monocular observation, one can only obtain the perpendicular velocity component v_{\perp} by assuming a distance. From the TUS height $H = 471$ [km] as this distance, it gives $v_{\perp} = H\omega \approx 79$ [km s $^{-1}$].

At the time of the event, TUS was heading $\sim 8^\circ$ west from the south, towards to the left along the x -axis of Panel (c). The light spot moved opposite to the heading angle. If the event was from a sporadic meteor, the velocity is below ~ 42 km s $^{-1}$, i.e., the escape velocity from the Sun's gravity near the Earth. As meteors occur at ~ 70 – 100 km heights, i.e., ~ 400 – 430 km away from TUS, it yields $v_{\perp} \lesssim 62$ km s $^{-1}$. The composite velocity v_T of the Earth's \vec{v}_{\oplus} and TUS' revolutions \vec{v}_S was ~ 31 km s $^{-1}$ in the counter direction. Thus, this motion does not contradict with a meteor.

For our setup, main observables are light curves and angular velocity. Unlike meteors, the light spot from nuclearites only monotonously varies its intensities by the change of distance r . The v_{\perp} component seen from the observer is given by $r\omega$. The 'absolute' velocity v_0 of a nuclearite in the Galaxy's frame is similar to its rotation velocity of ~ 229 km s $^{-1}$ near the Sun. The escape velocity limits v_0 below ~ 551 km s $^{-1}$. Sun's relative speed v_{\odot} to the Galactic Center is 246 km s $^{-1}$. These velocities [2] limit the 'relative' velocity below ~ 800 km s $^{-1}$ in the frame of the observer.

Figure 5 displays example light curves of moving-behavior events in the Level 0) data compared with those of the simulated 250 km s $^{-1}$ horizontally passing nuclearite event in Panel d). The TUS events are shown in Panels a): for selected channels of an event that almost all channels had saturated counts in a ~ 350 ms interval, b): three adjacent channels of a supposed stationary light event, and c): signals of six adjacent channels from a supposed meteor event.

As nuclearites may be seen as ‘fast’ moving events, we primarily analyzed how fast the most significant channel changed. In Level 0) data, we recognized that 226 events exhibited a moving behavior between channels with the maximum ADC counts with 25σ excesses. The Panel a) event is considered due to a stormy weather and light transient luminous event was responsible for simultaneous saturations. Three channels in Panel b) coincided the area near Schio, Italy. The peak time difference is 96 ticks (~ 0.63 s) to move over a plate scale. For $H = 479$ [km], the estimated v_{\perp} is 7.53 km s $^{-1}$ reasonable with the 7.65 km s $^{-1}$ ground speed of TUS. The Panel c) event is consistent with a meteor. The method used in Figure 4 gives $v_{\perp} \sim 39.8$ [km s $^{-1}$].

As in Panel d), nuclearite events may have much narrower time spreads of the signals and faster peak time shift between adjacent channels. We further cut those set of the events by the fastest peak channel shift faster than > 0.13 rad s $^{-1}$, i.e., $v_{\perp} \gtrsim 60$ [km s $^{-1}$]. The 76 events satisfied this criterion and then we applied a visible inspection on the remaining events. Within applied methods, no candidates of a moving light spot event consistent with nuclearites have been found.

5. Discussion and summary

To interpret the data and to estimate the performance of instrument we carried out a simulation study using radiation and detector models. To emulate the observation conditions, we checked the Level 2) criteria along the orbit every 5 s by calculating of the distance to the coast and Moon’s zenith angle. To estimate the observation ‘on-time’ time T_0 , we assumed that TUS was active for DAQ in any 5-s segment if the elapsed time after the last trigger was longer than 53 s. The first event after TUS entered the Earth’s umbra was excluded. By summing up these active segments, T_0 is estimated to be ~ 47.4 hours for Level 2). This also results in a trigger rate of ~ 0.49 min $^{-1}$.

Along the TUS orbit, there existed temporarily and locally clouds that could reduce the observation area and intensity of the light from the nuclearite. To include these effects, we employed MERRA2 (Modern-Era Retrospective analysis for Research and Applications, Version 2) [8]. It provides the global weather parameters outputs on 0.5° -latitude \times 0.625° -longitude-grid points.

Figure 6 displays the MERRA2-derived cloud-top-height (CTH; H_C) distribution on the Earth at 13:30 UTC of January 1st, 2017. Curves indicate TUS orbits between 08:35 and 19:35.

The H_C map is renewed every hour and the value is picked up every 5 s below the TUS position. To generate an artificial event from a nuclearite, we randomly sampled the conditions from all the active times to refer to H_C and the TUS height H and position. For an input mass of nuclearite m , the arrival direction and impact points are uniformly distributed onto the reference sphere with a radius R_0 beneath TUS. Among the generated N_{sim} events, the number of the events N_{sel} that overcome the event selection criteria gives an aperture A_0 by $2\pi^2 R_0^2 \cdot (N_{\text{sel}}/N_{\text{sim}})$.

Figure 7 summarizes the atmospheric profile models for air density $\rho(h)$ and ozone density [7] used for wavelength-dependent Rayleigh scattering and ozone absorption. The inset shows the H_C distribution. The limits of the density ρ_{th} and height H_{max} for effective radiation are marked for different masses. H_{max} has been modified from Reference [1] and became lower, e.g., by ~ 15 km at 1 kg. We generated the light from nuclearites in the heights $> H_C$ and $< H_{\text{max}}$.

We applied the ray trace and electronics response simulations with the background level and its fluctuation in ADC counts referred to the real data of the last event at the sampled time. For all channels and ticks, the background ADC counts are added by the Gaussian random generation.

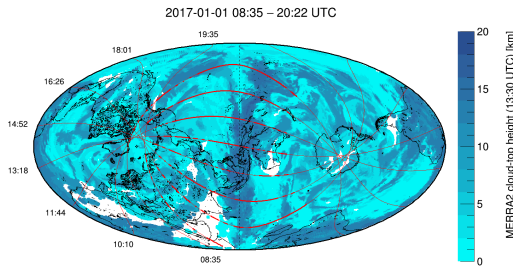


Figure 6: H_C map at 13:30 of January 1st, 2017. Curves shows a few of TUS orbits on that day .

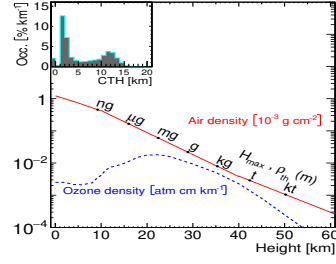


Figure 7: Atmospheric model, light generation limits for difference masses, and the H_C distribution.

SIMULATION (nuclearite m: 1.00e+03 [g]; $v = 250$ [km s⁻¹]) $\Theta_0: 73.8^\circ$ $\Phi_0: 96.7^\circ$ $v \sin \Theta_0: 240.1$ [km s⁻¹]
 ****-01-02 07:25:29UTC $\Theta_{\text{moon}} = 98.1^\circ$ CTH: 11.8 [km] $n_{\text{hit}} (>25\sigma) = 51$ $\omega_{\text{MD}}: +21.73$ [mrad s⁻¹] $\omega_{\text{PM}}: -508.28$ [mrad s⁻¹]
 H: 484.65 [km] Lat.: 15.19°N Long.: 126.63°W CD: 1812 [km] $\sum_{\text{PM}} n_{\text{hit}} (G=10^6) = 2.31e+05$ $\omega: 508.75$ [mrad s⁻¹] $v_{\text{H}}(H): 253.6$ [km s⁻¹]
 $v_{\text{MD}}: 7.68$ [km s⁻¹] $v_{\text{P}}: 32.05$ [km s⁻¹] $\alpha_{\text{P}}: 200.67^\circ$ $\delta_{\text{P}}: -14.71^\circ$ Preliminary Preliminary

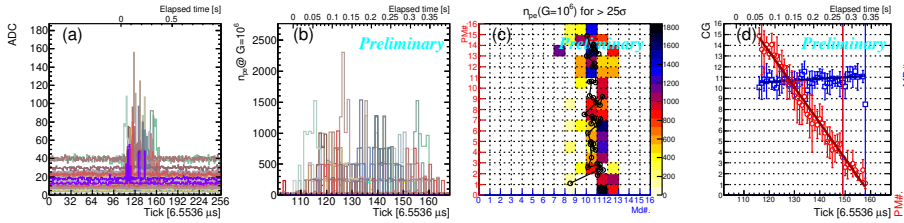


Figure 8: Selected example of a simulated nuclearite event. Panels are same as Figure 4.

Figure 8 displays a selected example of a simulated event from a 1 kg nuclearite at 250 km s^{-1} . Panels and applied analysis are same as in Figure 4.

To discriminate the nuclearite events from meteors and other moving events, many channels with significant signals are desired to determine the angular velocity and light curve property. To estimate a sensitivity in terms of ‘aperture’ of such an analysis, we applied relatively tight cuts on simulated events. In addition to Level 2) conditions, we required 2a) ≥ 10 channels with the maximum ADC counts above 25σ and 2b) ≥ 10 ticks (~ 66 ms) available for the motion analysis.

Table 1 summarize the preliminary results on the aperture A_0 for Conditions 2a) and 2b), and qualities of angular velocity ω and orientation Ψ for 2b) as of the root mean square (RMS) of the errors. Combinations of 100 g, 10 and 100 kg, and $v=75, 250$, and 800 km s^{-1} were simulated.

Due to v and m are both unknown parameters, and there are uncertainties of the estimated gain, we only show the values for the nuclearite above 100 g where the results are stable. Taking into account the $T_0 \sim 2$ [day] on-time, our sensitivity $\sim 1/(A_0 \cdot T_0)$ to the nuclearite flux was found above the limit complied with the dark matter density.

As a short remark on the future perspectives, the basic techniques developed in the present work may apply to similar experiments. As of the lowest v in these simulations was chosen for that of the fastest meteors that can mimic nuclearite events. Angular velocity ω is a key parameter to evaluate possible nuclearite velocity. Apart from RMS in the table, the retrieved ω tends to be lower due to the tick duration optimized to the meteor. Indeed, Panel c) event of Figure 5 was observed with the time peak night of the Quadrantids meteor shower. Its radiant and velocity were

Table 1: Preliminary results of the estimated apertures A_0 for Conditions 2a) and 2b) and qualities of the analyzed angular velocity ω and orientation Ψ for 2b). Different combinations of v and m are simulated.

v [cm s ⁻¹] m [g]	2a): A_0 [10 ¹⁴ cm ² sr]			2b): A_0 [10 ¹⁴ km ² sr]			$\sqrt{\langle(\Delta\omega/\omega)^2\rangle}$			$\sqrt{\langle(\Delta\Psi)^2\rangle}$		
	10 ²	10 ³	10 ⁵	10 ²	10 ³	10 ⁵	10 ²	10 ³	10 ⁵	10 ²	10 ³	10 ⁵
800	1.3	2.6	3.2	0.07	0.2	0.7	–	–	0.08	–	–	7.4°
250	0.3	0.9	2.0	0.1	0.6	1.5	0.08	0.29	0.33	14°	22°	30°
75	0.4	0.6	1.0	0.2	0.3	0.8	0.52	2.1	0.40	58°	39°	48°

consistent with the Ψ angle and ω value of this event. It should be noted that a 6.6 ms of the METEOR mode tick consisted of 8192 ‘EAS mode’ ticks of a 0.8 μ s resolution. Another ‘‘TLE’’ mode was operated at a 0.4 ms tick duration. Thus, electronics itself could be tuned for nuclearites.

In the present work, the main task was the estimation of ‘exposure’, we assumed the nuclearite flux at the various relative velocity v and ‘constant intensity’ on the reference sphere and estimated the aperture estimation by the ratio of selected events for. It is a commonly accepted technique by the EAS experiments. On the other hand, it is highly unlikely that the flux of the nuclearites are isotropic in our frame. In the frame of the Galaxy, an absolute velocity v_0 is seen to be $v = \vec{v}_0 - (\vec{v}_\odot + \vec{v}_\oplus + \vec{v}_T)$. The dominant component is the Sun’s velocity \vec{v}_\odot to the Galaxy and then the Earth’s to the Sun. These effects in anisotropic fluxes may be convoluted to the apertures calculated in the finer v intervals. In the TUS orbit, these vectors, the effect of clouds, the background level, and the observation time were estimated using various tools. This approach may be used for the study of not only the nuclearite search but also for the supplementary information for the satellite-based UHECR observation.

Acknowledgments

The Italian group acknowledges financial contributions from the agreement ASI-INAF n.2017-14-H.O and Italian Ministry of Foreign Affairs and International Cooperation. The present work has been performed with partial financial support from the State Space Corporation ROSCOSMOS, M.V. Lomonosov Moscow State University through its ‘‘Prospects for Development’’ program and the Russian Foundation for Basic Research grant No. 16-29-13065 and 15-02-05498/17-a.

References

- [1] A. De Rújula and S.L. Glashow, Nature 312 (1984) 734.
- [2] P.R. Kafle, S. Sharma, G.F. Leis, and J.Bland-Hawthorn, Astrophys. J. 794 (2014) 59.
- [3] P.B. Price, Phys. Rev. D 38 (1988) 3813.
- [4] MACRO Collaboration, M. Ambrosio et al., Eur. Phys. J. C13 (2000) 453.
- [5] G.E. Pávlař et al., Proc. 34th Int. Cosmic Ray Conf., Pos (ICRC2015) 1060.
- [6] P.A. Klimov et al., Space Sci. Rev. 212 (2017) 1687.
- [7] F.X. Kneizys et al., ‘‘The MODTRAN 2/3 Report and LOWTRAN 7 Model’’ (1996).
- [8] Global Modeling and Assimilation Office, <https://gmao.gsfc.nasa.gov/pubs/docs/Bosilovich785.pdf>